VERTEBRATE ZOOLOGY

69 (2): 145–160
2019

SENCKENBERG

A new species of anole from the Sierra Madre del Sur in Guerrero, Mexico (Reptilia, Squamata, Dactyloidae: *Norops*)

Gunther Köhler[1], Claus Bo P. Petersen[1] & Fausto R. Méndez de la Cruz[2]

[1] Senckenberg Forschungsinstitut und Naturmuseum, Senckenberganlage 25, 60325 Frankfurt a. M., Germany; gkoehler@senckenberg.de — [2] Instituto de Biología, Universidad Nacional Autónoma de México (UNAM), A.P. 70-153, C.P. 04510, México D.F., México; faustomendez6@gmail.com

Submitted November 11, 2018.
Accepted March 15, 2019.
Published online at www.senckenberg.de/vertebrate-zoology on March 28, 2019.
Published in print on Q2/2019.

Editor in charge: Uwe Fritz

Abstract

We describe the new species *Norops brianjuliani* sp. nov. from the Pacific versant of southern Mexico. *Norops brianjuliani* differs from all congeners by having a combination of (1) smooth ventral scales; (2) usually a patch of three greatly enlarged supraocular scales; (3) moderately long hind legs, longest toe of adpressed hind leg reaching to a point between posterior and anterior levels of eye, ratio shank length/snout-vent length 0.24–0.26; (4) a pair of greatly enlarged postcloacal scales in males; (5) 10 to 12 rows of greatly enlarged, keeled middorsal scales; and (6) a large pink dewlap in males. In external morphology, *N. brianjuliani* is most similar to *N. liogaster* from which it differs by having larger middorsal scales (more than three times the size of granular flank scales in *N. brianjuliani* vs. less than three times in *N. liogaster*). Also, in a preliminary molecular genetic analysis, *N. brianjuliani* has a genetic distance of 8.7% (16S) and 15.3% (COI), respectively, from *N. liogaster*.

Resumen

Describimos la nueva especie *Norops brianjuliani* de la vertiente Pacífico del sureste de México. *Norops brianjuliani* difiere de todos sus congéneres al tener una combinación de (1) escamas ventrales lisas; (2) usualmente un parche de tres escamas supraoculares fuertemente agrandadas; (3) patas traseras moderadamente largas, cuando la pata posterior está adpresa al cuerpo, el cuarto dedo alcanza un punto entre el nivel posterior y anterior del ojo, proporción de la longitud de la pierna/longitud hocico-cloaca 0.24–0.26; (4) un par de escamas postcloacales muy agrandadas en machos; (5) 10 a 12 hileras de escamas mediodorsales muy agrandadas y quilladas; y (6) presencia de un gran abanico gular rosado en machos. En morfología externa, *N. brianjuliani* es más similar a *N. liogaster* del cual se diferencia por tener escamas mediodorsales más agrandadas (más de tres veces el tamaño de las escamas granulares laterales en *N. brianjuliani* vs. menos de tres veces el tamaño en *N. liogaster*). Además, en un análisis preliminar de genética molecular, *N. brianjuliani* presenta una distancia genética de 8.7% (16S) y 15.3% (COI), respectivamente, de *N. liogaster*.

Key words

Norops brianjuliani **sp. nov.**; Dactyloidae; Mexico; new species; Guerrero; Reptilia; Squamata.

Introduction

Southern Mexico (states of Chiapas, Oaxaca, and Guerrero) supports a rich herpetofauna with the beta anoles (genus *Norops*) forming a prominent component among the reptiles. The species of anoles occurring along the Pacific versant of the Sierra Madre del Sur in the Mexican States of Oaxaca and Guerrero have been reviewed by Köhler *et al*. (2014a) who recognized 21 species in this region. Already at that time we had specimens of a *No-*

rops liogaster-like anole from near Espino Blanco, Sierra Madre del Sur, Guerrero, Mexico, that did not seem to be conspecific with any of the then recognized species. We have completed a comparison of external morphology and molecular data of the Espino Blanco specimens with that for all known Mexican and Central American species of *Norops*, which confirmed our initial assumption that the Espino Blanco population represents an undescribed species. Therefore, we describe it as a new species below.

We are aware of the contentious debate between recognizing *Anolis* as a single genus and recognizing multiple genera (see Poe, 2004; Nicholson *et al*., 2012, 2014; Castañeda & de Queiroz, 2013; Poe, 2013; Poe *et al*., 2017; Nicholson *et al*., 2018). Here we refer to the monophyletic grouping of beta anoles as *Norops* (sensu Nicholson *et al*., 2018), while recognizing the criticisms of the multiple-genera taxonomy. The genus *Norops* sensu Nicholson *et al*. (2018) corresponds to clade *Norops* of Poe *et al*. (2017), and the species it contains all share the synapomorphy of anterolaterally directed transverse processes on their caudal vertebrae (Etheridge, 1959) as well as numerous molecular characters (Poe, *et al*., 2017; Nicholson *et al*., 2018).

Materials and methods

Specimens examined for this study were either personally collected or borrowed from museums (see Appendix 1 for specimens examined). In evaluating species boundaries within the populations of anoles found in western Mexico, we follow the unified species concept (de Queiroz, 2007). As lines of evidence for species delimitation, we apply a phenotypic criterion (external morphology: coloration, morphometrics, and pholidosis) and a criterion for reproductive isolation (genetic distinctness of the mitochondrial genes 16S rRNA and Cytochrome Oxidase Subunit I, COI).

Prior to preservation of collected specimens in the field, we took color photographs of each individual's extended dewlap. Immediately after euthanasia, relative hind limb length was determined by recording the point reached by the tip of the fourth toe when the extended hind limb was adpressed along the straightened specimen. Whenever possible, we everted the hemipenes of male specimens by injecting 70% ethanol into the hemipenial pockets after manually pre-everting the hemipenes. Specimens were then preserved by injecting a solution of 5–10 mL absolute (i.e., 36%) formalin in 1 L of 96% ethanol into the body cavity and thighs, preferably also sprinkling everted hemipenes and extended dewlaps with this solution, and stored in 70% ethanol. The collected specimens have been deposited in the collection of the Senckenberg Forschungsinstitut Frankfurt (SMF), and in the collection of the Instituto de Biología (IBH), Universidad Nacional Autónoma de México (UNAM), México D.F., Mexico. Abbreviations for museum collections follow Sabaj Pérez (2016). Coordinates and elevation were recorded using Garmin GPS receivers with built-in altimeters. All coordinates are in decimal degrees, WGS 1984 datum. The capitalized colors and color codes (the latter in parentheses) are those of Köhler (2012) in the color descriptions. We followed Köhler (2012) for the terminology of markings used in the color descriptions, and used Köhler (2014) for nomenclature and definitions of morphological characters. Abbreviations used are AGD (axilla-groin distance), dorsAG (number of medial dorsal scales between levels of axilla and groin), dorsHL (number of medial dorsal scales in one head length), HDT (horizontal diameter of tail), HL (head length), HW (head width), IFL (infralabials), IP (interparietal plate), SAM (scales around midbody), ShL (shank length), SL (snout length), SO (subocular scales), SPL (supralabial scales), SS (supraorbital semicircles), SVL (snout–vent length), TL (tail length),VDT (vertical diameter of tail), ventrAG (number of medial ventral scales between levels of axilla and groin), and ventrHL (number of medial ventral scales in one head length). To measure dewlap area, we took photographs of males in life with their dewlaps artificially extended using small forceps. The head portion was magnified and printed and then superimposed on millimetric paper; the total number of millimeter squares contained in the extended dewlap was counted. A straight line was drawn between the anterior and posterior insertions of the dewlap. The HL on the printout was also determined. We used the following equation to convert the magnified dewlap area to the real size: $X = [(\sqrt{Y}/A)B]^2$, where × is the real area of the dewlap in square millimeters, Y is the total area (square millimeters) of the dewlap at a magnified scale, A is the HL measure (millimeters) of the anole at a magnified scale, and B is the HL measure (millimeters) of the anole at the real size. Sex of the subadult paratypes was determined on the basis of presence versus absence of a pair of greatly enlarged postcloacal scales, which are only present in males.

We cut tissue samples from the tip of the tail or the tongue of selected individuals before they came into contact with formalin. The tissue samples were deposited in the collection of the Senckenberg Forschungsinstitut und Naturmuseum, Frankfurt, Germany. We extracted DNA following the protocol of Ivanova *et al*. (2006). To eliminate potential PCR-inhibiting contaminants, the tissue samples were incubated for 14 hrs at 4°C in 200 µL low PBS buffer (20 µL PBS in 180 µL of water) before overnight digestion with the vertebrate lysis buffer at 56°C. After extraction, the DNA was eluted in 50 µL TE buffer. A fragment of the mitochondrial 16S rRNA gene (specifications for COI in parentheses) was amplified in an Eppendorf Mastercycler® pro using the following protocol: initial denaturation for 2 min (1.5 min) at 94°C; followed by 40 (37) cycles with denaturation for 35 s (40 s) at 94°C, hybridization for 35 s (40 s) at 48.5°C (45°C), and elongation for 60 s (40 s) at 72°C; final elongation for 10 min (6 min) at 72°C. The reaction mix for each sample contained 1 µL DNA template, 14 µL water, 2.5 µL PCR-buffer, 1 µL 25 mM $MgCl_2$, 4 µL 2.5 mM dNTPs (Invitrogen), 0.5 µL (containing 2.5 units) Taq

Polymerase (PeqLab), and 1 µL of each primer (16S: forward: L2510, 5'–CGCCTGTTTATCAAAAACAT–3'; reverse: H3056, 5'–CCGGTCTGAACTCAGATCACGT–3'; COI: forward: dgLCO-1490, 5'–GGTCAACAAAT CATAAAGAYATYGG–3'; reverse: dgHCO-2198, 5'–TAAACTTCAGGGTGACCAAARAAYCA–3'; both from Eurofins MWG Operon).

We aligned the sequences with MUSCLE (EDGAR, 2004) using the default settings in GENEIOUS 6.1.2 (DRUMMOND *et al*., 2010). Using MEGA 6 (TAMURA *et al*., 2013), we computed uncorrected pairwise genetic distances, determined T92 + G + I as the best-fitting substitution model, and conducted a Maximum Likelihood (ML) analysis with 10,000 bootstrap replicates and gaps as a fifth character (i.e., using all sites). In evaluating the uncorrected *p*-distances calculated for our sample, we follow other recently published barcoding studies on Central American and Mexican anoles (LOTZKAT *et al*., 2011; KÖHLER *et al*., 2012; KÖHLER *et al*., 2014a,b, 2016).

According to the respective requirements of the different software applications, the formats of the sequences were converted using the online server Alter (GLEZ-PEÑA *et al*., 2010). The best substitution model for each gene (analyzed separately) of our dataset was identified using PartitionFinder2 (LANFEAR *et al.,* 2016), with linked branch lengths (supported by most of the phylogenetic programs) via PhyML 3.0 analysis (GUINDON *et al*., 2010). Model selection was detected using the corrected (for finite sample size) Akaike Information Criterion (AICc) (BURNHAM & ANDERSON, 2002). Given the correlation between gamma (+ G) and invariant sites (+ I) parameters, models that include both + G and + I are often inadequate (SULLIVAN, *et al*., 1999; MAYROSE *et al*., 2005; YANG, 2006). Thus, we did not use models that included both parameters together. In all analyses, we used the *Basiliscus vittatus* mitogenome (GenBank AB218883) as an outgroup. All of the following analyses were conducted for each gene individually, and the two genes concatenated. Sequences were concatenated in Geneious 6.1.2 (DRUMMOND *et al*., 2010). We performed Bayesian Inference analysis (BI) with MRBAYES 3.2 (HUELSENBECK & RONQUIST, 2001; RONQUIST & HUELSENBECK, 2003). BI analyses were performed setting 5 runs with 8 chains discarding the first 25% as the burn-in period and an initial set of 1,000,000 generations for MCMC with a sampling frequency of 500 generations, adding 500,000 generations until chains reached convergence. We considered convergence when the standard deviation of split frequencies was 0.015 or less. Additionally, convergence was diagnosed by PRSF (Potential Scale Reduction Factor) which should approach 1.0 as runs converge (GELMAN & RUBIN, 1992). We used the IQTree webserver (TRIFINOPOULOS *et al*., 2016) to run a Maximum Likelihood (ML) analysis using 10,000 ultrafast Bootstrap approximation (UFBoot) replicates with 10,000 maximum iterations and minimum correlation coefficient of 0.99 (MINH *et al*., 2013) plus 10,000 replicates of Shimodaira-Hasegawa approximate likelihood ratio (SH-aLRT), which proved to be accurate with a high statistical power (GUINDON *et al*., 2010). We used FigTree 1.3.1 for tree viewing (http://tree.bio.ed.ac.uk/software/figtree/). We estimated evolutionary genetic divergence, computing uncorrected pairwise distances with MEGA 7.0.26 (KUMAR *et al*., 2016) to assess the degree of intra and interspecific differences, using a Bootstrap estimation method of 10,000 replications. To assess the phylogenetic position of the the Espino Blanco population, we designed a species tree based on the two mtDNA gene sequences concatenated, using *BEAST (DRUMMOND *et al*., 2012) in BEAST 2.4.7 (OGILVIE *et al*., 2017) under 1,000,000 generations for the mcmc model, visualizing the posterior probability in DENSITREE 2.2.6 (BOUCKAERT & HELED, 2014). We performed an initial species delimitation analysis by visualizing barcode gaps in the pairwise distribution of each mtDNA gene separately (excluding the outgroup), using the automatic barcode gap discovery (ABGD) approach (PUILLANDRE *et al*., 2012) through its webserver (http://wwwabi.snv.jussieu.fr/public/abgd/abgdweb.html), setting the use of Simple Distance, default values for Prior Intraspecific divergence, except for relative gap width (1.5) which does not work for some genes (as also noted by KEKKONEN *et al*., 2015). Because high values in relative gap width tend to overly split species (YANG *et al*., 2016), we used an intermediate value of 0.9.

Results

The final alignments of 16S and COI were of 589 and 677 nucleotide positions, respectively, for 66 *Norops* samples plus *Basiliscus vittatus* as an outgroup (Appendix 2). Partition schemes were recorded as follows: 16S (GTR+G); COI (1st pos TIM+I |2nd pos TIM+I |3rd pos TIMEF+I). The trees obtained through BI, ML, *BEAST, and ABGD showed a high degree of congruence at well-supported nodes, with some differences in branch arrangement at poorly supported nodes (Fig. 1 and 2). In particular, the Espino Blanco specimens are always included in a clade containing also the species *N. dunni, N. taylori*, and *N. liogaster*. The clade of the Espino Blanco specimens clustered as the sister taxon of *N. liogaster* in *BEAST, but is basal to a clade containing *N. dunni, N. taylori*, and *N. liogaster* in ML and BI.

Results from the ABGD analysis show a similar tree topology as the analyses mentioned above and also support the recognition of the Espino Blanco population as a distinct species.

The results of our analyses of the single markers as well as the concatenated alignments indicate a high degree of genetic differentiation of the Espino Blanco population. The genetic distances between specimens from near Espino Blanco and its most closely related species are as follows (in parentheses values for 16S/COI, respectively), in order of increasing genetic distance: *N. liogaster* (8.7% / 15.37%), *N. taylori* (10.2% / 17.6%), *N. dunni* (10.7% / 17.5%). We interpret the high degree of genetic distinctiveness among the Espino

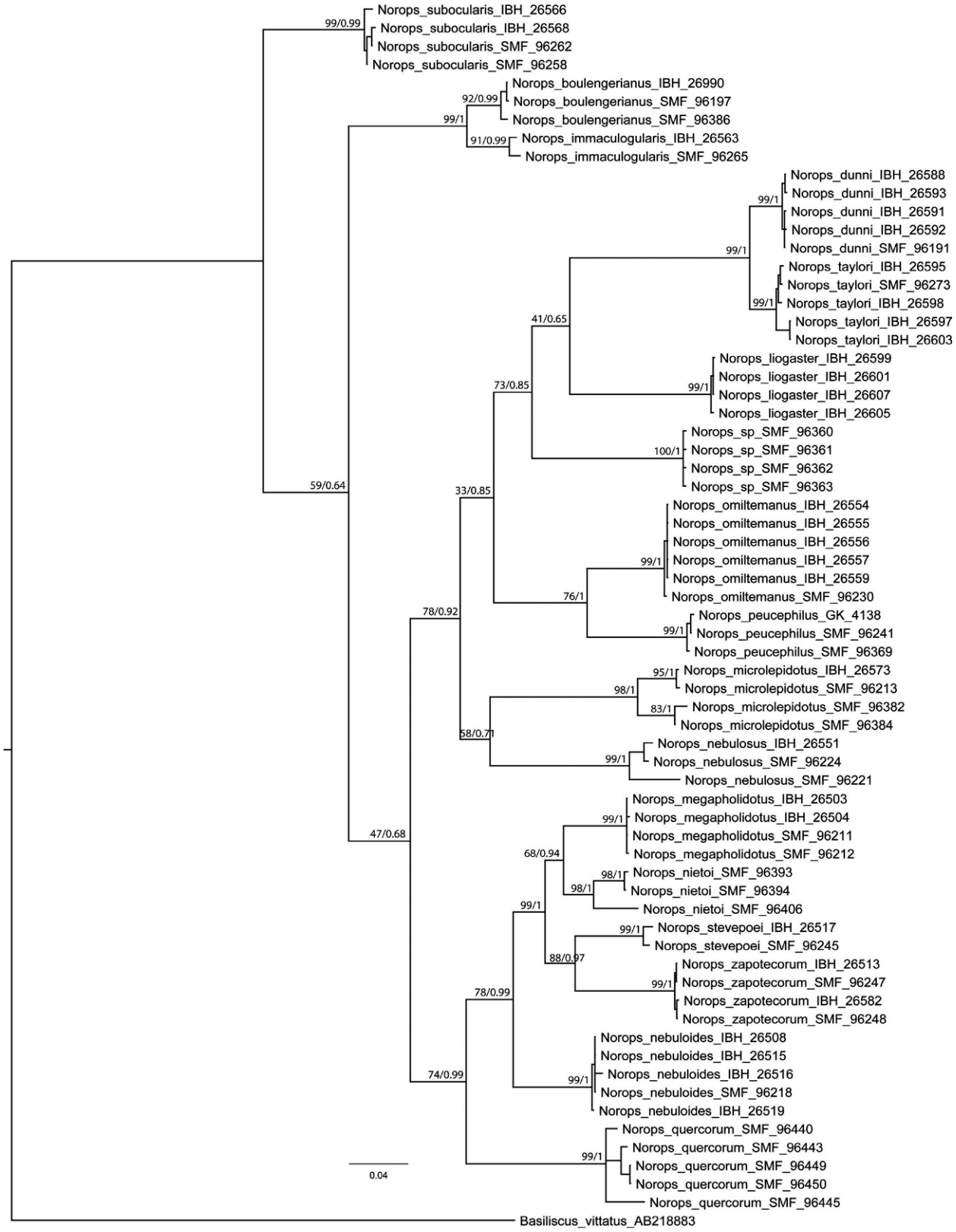

Fig. 1. Phylogenetic tree of specimens of the genus *Norops*, species from the Pacific versant of southern Mexico, from a maximum-likelihood analysis of DNA sequences of two mitochondrial genes: 16S and COI. The numbers at nodes are bootstrap values (left) and Bayesian posterior probabilities (right). The tree is rooted with the species *Basiliscus vittatus* (GenBank AB218883).

Blanco population as evidence for genetic isolation, and conclude that it represent a species-level unit, distinct from *N. liogaster*, *N. taylori*, and *N. dunni*. In morphology the Espino Blanco population is most similar to *N. liogaster*, with which it shares having several rows of enlarged dorsal scales and a large uniformly pink dew-

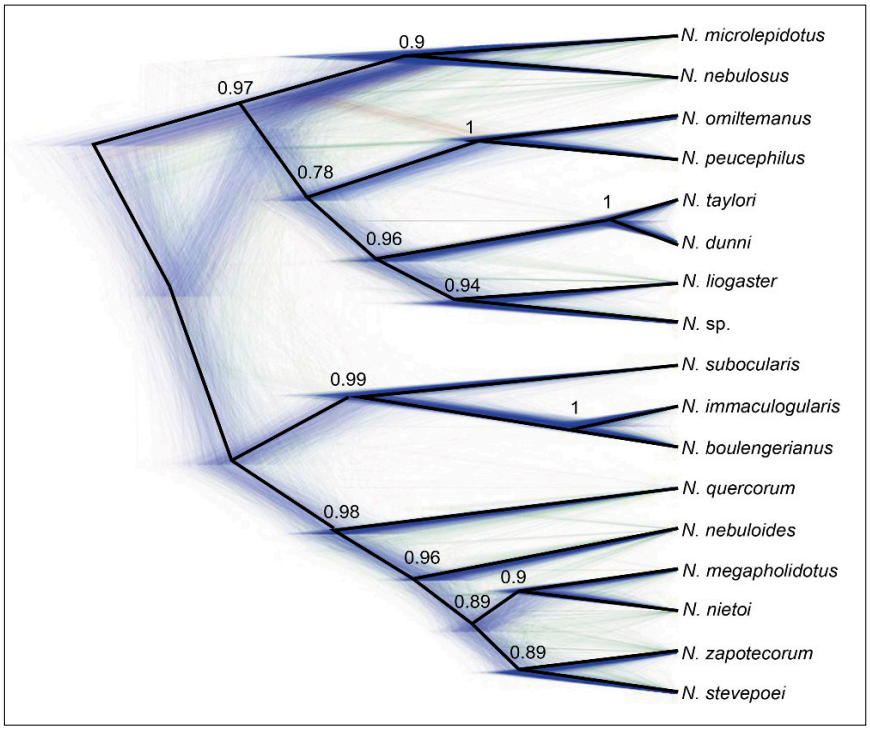

Fig. 2. Species tree inferred with ∗BEAST showing density of trees proportional to frequency of occurrence (thin lines) drawn in DENSITREE and the consensus tree (black lines) with the posterior probability for each node.

lap in adult males (versus middorsal scales only slightly enlarged and a pinkish to orange-red male dewlap with semicircular pale streaks and blotches in *N. taylori*, and *N. dunni*). Individuals of the Espino Blanco population differ from *N. liogaster* by having even larger middorsal scales (more than three times the size of granular flank scales vs. less than three times in *N. liogaster*; Fig. 3). Furthermore, the Espino Blanco population differs from *N. liogaster* in the mean values of other characters of external morphology, further supporting the recognition of each of these as a distinct species (Table 1, Fig. 4). Since no scientific name is available for our Espino Blanco population of *N. liogaster*-like anoles, we describe them as a new species below.

Norops brianjuliani sp. nov.

ZooBank urn:lsid:zoobank.org: act: DECA719E-57B4-4BE0-B011-BCF0E8522F23

Figs 3a, 5 – 7

Holotype. SMF 96360, an adult male from near Espino Blanco, along road from Santa Cruz El Rincón to Tlapa (17.10336°N, 98.73065°W, WGS84), 2055 m, Estado de Guerrero, Mexico; collected 11 January 2013 by Raúl Gómez Trejo Pérez. Field tag number GK-4240.

Paratypes. SMF 96361 – 63, same collecting data as holotype. All paratypes are subadults, SMF 96362 is a male, SMF 96361 and 96363 are females.

Diagnosis. A small to moderate-sized species (SVL in single known adult male 50.0 mm, no adult female known) of the genus *Norops* (sensu NICHOLSON *et al*., 2018) that differs from all other Mexican and Central American congeners except *N. dunni, N. gadovii, N. liogaster, N. omiltemanus,* and *N. peucephilus* by having (1) smooth ventral scales; (2) an oval patch of usually three greatly enlarged supraorbital scales; (3) a pair of greatly enlarged postcloacal scales in males; (4) a large, uniform pink dewlap in adult males (Fig. 5). *Norops brianjuliani* differs from *N. dunni* and *N. gadovii* by having 10 – 12 rows of dorsal scales greatly enlarged (vs. the middorsal scales not or only 2 – 4 rows slightly enlarged in *N. dunni* and *N. gadovii*). It further differs from *N. dunni* by having a uniform purple to pink male dewlap (vs. pinkish to orange red male dewlap with semicircular pale streaks and blotches in *N. dunni*). It also differs from *N. gadovii* by the absence of a bold reticulated body pattern (vs. such a pattern present in *N. gadovii*). *Norops brianjuliani* differs from *N. omiltemanus* and *N. peucephilus* by having longer hind legs with the longest toe of adpressed hind leg reaching to a point between posterior and anterior margin of eye or occasionally to a point between ear opening and eye (vs. to level of ear opening or to a point between shoulder and ear opening in *N. omiltemanus* and *N. peucephilus*), usually only a single pair of greatly enlarged sublabial scales in contact with infralabial scales (vs. usually two pairs in *N. omiltemanus* and *N. peucephilus*), and a pink to purple male dewlap (vs. orange yellow in *N. omiltemanus* and *N. peucephilus*). *Norops brianjuliani* differs from *N. liogaster* by having larger middorsal scales (more than three times the size of granular flank scales in *N. brianjuliani* vs. less than three times in *N. liogaster*).

Description of the holotype (Figs. 5 – 7). Adult male, as indicated by everted hemipenes and presence of large

Table 1. Selected measurements, proportions and scale characters of *Norops liogaster* and related species. Range is followed by mean value and standard deviation in parentheses. For abbreviations see text.

		Norops dunni ♂ 25 | ♀ 14	***Norops taylori*** ♂ 30 | ♀ 19	***Norops liogaster*** ♂ 19 | ♀ 22	***Norops brianjuliani*** ♂ 2 | ♀ 2
maximum SVL	males	58.5	73.0	50.0	50.0
	females	51.0	58.0	54.0	29.0 (subadult)
TL / SVL	males	1.75–2.09 (1.92±0.10)	1.95–2.11 (2.02±0.06)	1.90–2.27 (2.08±0.14)	
	females	1.86–1.97 (1.90±0.04)	1.94–2.16 (2.03±0.08)	1.75–2.07 (1.93±0.14)	
VDT / HDT	males	1.13–1.48 (1.31±0.10)	1.17–1.70 (1.52±0.13)	1.16–1.50 (1.28±0.09)	1.32
	females	1.19–1.60 (1.35±0.14)	1.17–1.44 (1.33±0.08)	1.05–1.59 (1.26±0.15)	
AGD / SVL	males	0.37–0.44 (0.40±0.02)	0.37–0.44 (0.40±0.02)	0.34–0.45 (0.40±0.03)	0.41–0.42 (0.42±0.01)
	females	0.38–0.46 (0.42±0.02)	0.41–0.46 (0.43±0.01)	0.38–0.47 (0.42±0.02)	0.38–0.40 (0.39±0.01)
HL / SVL	males	0.24–0.28 (0.27±0.01)	0.23–0.29 (0.26±0.01)	0.27–0.33 (0.29±0.01)	0.27–0.28 (0.28±0.01)
	females	0.25–0.28 (0.26±0.01)	0.24–0.28 (0.26±0.01)	0.25–0.29 (0.28±0.01)	0.28–0.29 (0.29±0.01)
HL / HW	males	1.53–1.76 (1.67±0.06)	1.60–1.84 (1.72±0.07)	1.59–1.75 (1.66±0.05)	1.65–1.67 (1.66±0.02)
	females	1.58–1.80 (1.69±0.05)	1.61–1.86 (1.73±0.06)	1.46–1.69 (1.60±0.06)	1.62–1.67 (1.64±0.03)
SL / SVL	males	0.11–0.13 (0.11±0.01)	0.11–0.13 (0.11±0.01)	0.12–0.15 (0.13±0.01)	0.11–0.12 (0.12±0.01)
	females	0.10–0.13 (0.12±0.01)	0.11–0.13 (0.12±0.01)	0.11–0.13 (0.12±0.01)	0.11–0.12 (0.12±0.01)
SL / HL	males	0.42–0.46 (0.44±0.01)	0.43–0.48 (0.45±0.01)	0.42–0.47 (0.44±0.02)	0.40–0.45 (0.42±0.03)
	females	0.42–0.46 (0.44±0.01)	0.43–0.48 (0.45±0.02)	0.42–0.46 (0.44±0.01)	0.41
ShL / SVL	males	0.24–0.29 (0.26±0.01)	0.24–0.32 (0.26±0.02)	0.25–0.30 (0.27±0.01)	0.24–0.26 (0.25±0.01)
	females	0.24–0.27 (0.25±0.01)	0.24–0.30 (0.26±0.01)	0.24–0.28 (0.26±0.01)	0.24–0.25 (0.25±0.01)
ShL / HL	males	0.88–1.03 (0.97±0.04)	0.95–1.12 (1.03±0.04)	0.84–1.05 (0.93±0.06)	0.85–0.95 (0.90±0.07)
	females	0.88–1.00 (0.94±0.04)	0.88–1.10 (0.99±0.05)	0.87–1.04 (0.93±0.04)	0.85–0.87 (0.86±0.01)
dorsHL	males	32–48 (40.4±5.0)	38–52 (44.2±4.2)	22–36 (27.5±3.2)	24–26 (25.0±1.4)
	females	26–42 (37.2±4.4)	36–54 (41.5±4.4)	22–34(28.5±3.0)	23–30 (26.5±4.9)
ventrHL	males	32–44 (37.3±3.6)	38–60 (50.3±5.7)	24–38 (28.5±4.1)	22–26 (24.0±2.8)
	females	22–40 (28.4±5.1)	28–46 (33.8±4.4)	18–28 (23.6±3.0)	26–28 (27.0±1.4)
dorsAG	males	58–80 (71.2±7.0)	69–101 (81.0±7.2)	37–58 (47.7±6.6)	43
	females	51–80 (70.8±8.4)	72–105 (84.8±8.0)	44–65 (52.9±6.1)	44–57 (50.5±9.2)
ventrAG	males	46–64 (55.4±4.4)	56–73 (67.7±4.5)	35–47 (40.5±3.9)	40–41 (40.5±0.7)
	females	37–61 (51.0±6.6)	50–72 (59.5±6.2)	33–45 (40.2±3.0)	42–45 (43.5±2.1)
SAM	males	122–162 (147.6±11.9)	156–188 (175.1±9.1)	102–128 (115.4±7.5)	108–122 (115.0±9.9)
	females	118–150 (137.1±10.1)	150–168 (159.0±6.4)	92–132 (113.4±11.0)	116–118 (117.0±1.4)
subdigital lamellae on Phalanges II–IV of Toe IV		22–29 (26.0±1.8)	25–32 (28.8±1.9)	20–28 (24.4±2.2)	22–25 (23.5±1.2)
subdigital lamellae on distal phalanx of Toe IV		5–8 (6.8±0.8)	6–9 (7.4±0.6)	6–9 (6.7±0.7)	7–8 (7.3±0.5)
number of scales between SS		0	0	0–1 (0.2±0.4)	0–1 (0.3±0.5)
number of scales between IP and SS		0–3 (1.3±0.6)	0–3 (1.4±0.6)	1–3 (1.9±0.5)	1–2 (1.8±0.5)
number of scales between SO and SPL		0	0	0	0
number of SPL to level below center of eye		5–8 (6.4±0.6)	5–9 (6.7±0.6)	5–7 (5.6±0.6)	5–6 (5.9±0.4)
number of IFL to level below center of eye		5–7 (5.7±0.6)	5–8 (6.3±0.6)	5–7 (5.6±0.6)	5–7 (5.9±0.6)
total number of loreals		18–36 (25.7±4.5)	19–42 (31.2±5.7)	16–39 (24.8±5.7)	21–28 (24.7±2.7)
number of horizontal loreal scale rows		4–6 (4.9±0.5)	4–6 (5.6±0.6)	4–6 (4.8±0.6)	4–6 (5.3±0.7)
number of postrostrals		5–6 (5.3±0.5)	5–7 (5.9±0.6)	5–8 (5.9±0.7)	5
number of postmentals		2–6 (4.1±0.6)	4–7 (4.3±0.7)	2–5 (3.9±0.5)	3–4 (3.5±0.6)
number of sublabials		1–2 (1.0±0.1)	1–2 (1.2±0.4)	0–2 (1.0±0.2)	1–2 (1.4±0.3)
number of scales between nasals		6–8 (6.8±0.6)	7–9 (7.6±0.6)	6–8 (6.9±0.7)	6–7 (6.5±0.6)

Table 1 continued.

number of moderately to greatly enlarged supraoculars	3–5 (3.5±0.6)	3–6 (3.6±0.7)	2–6 (3.4±1.0)	3–4 (3.4±0.5)
number of scales between 2nd canthals	5–9 (6.2±1.1)	4–9 (6.1±1.0)	4–9 (5.5±0.9)	5–6 (5.3±0.5)
number of scales between posterior canthals	7–10 (8.4±0.9)	6–12 (9.3±1.3)	5–11 (7.2±1.4)	7–8 (7.8±0.5)
number of rows of enlarged dorsal scales	2–6 (4.2±1.3)	2–6 (3.5±1.4)	10–17 (13.1±2.1)	10–12 (11.3±1.0)

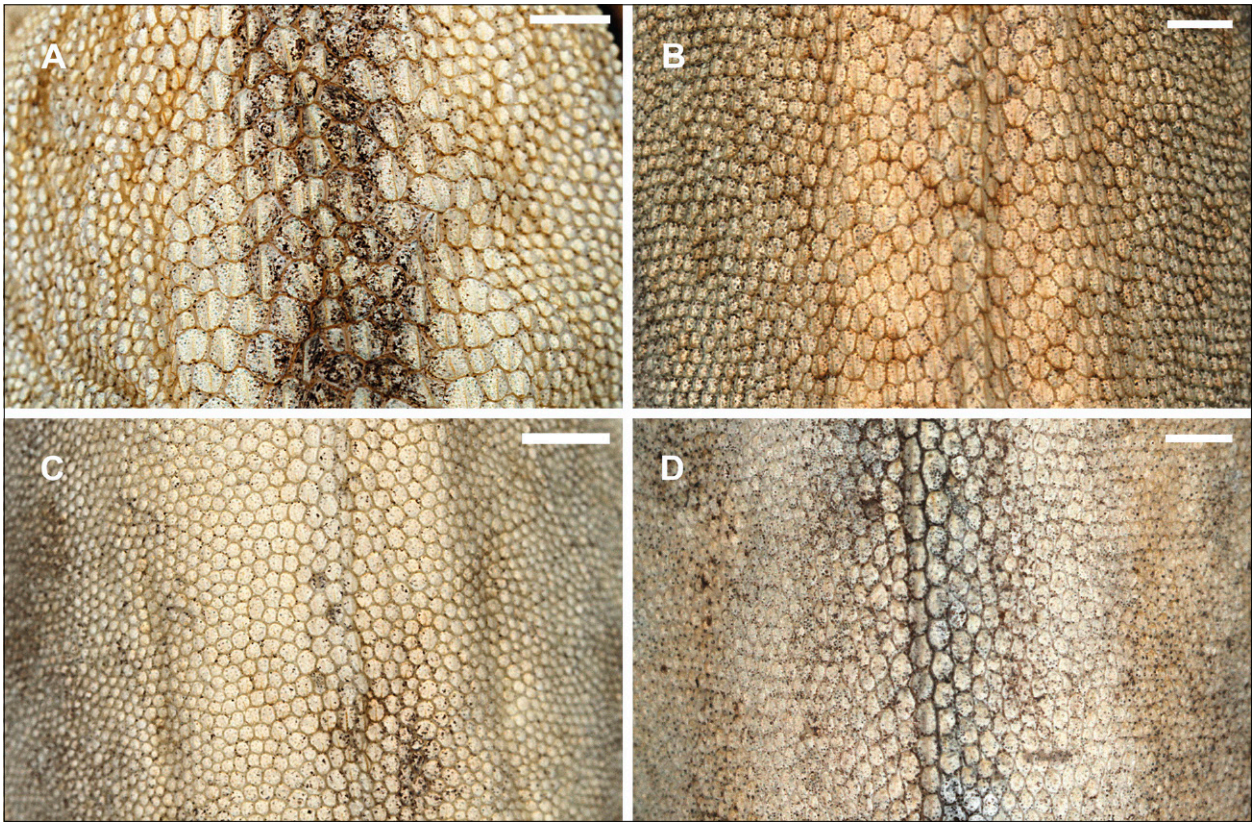

Fig. 3. Dorsal scalation in (A) *Norops brianjuliani* (SMF 96360); (B) *N. liogaster* (SMF 96202); (C) *N. dunni* (SMF 96380); (D) *N. taylori* (SMF 96271). Scale bars equal 1.0 mm. Photos by G.K.

dewlap; SVL 50.0 mm; tail incomplete; tail slightly compressed in cross section, tail height 2.5 mm and width 1.9 mm; axilla to groin distance 21.2 mm; head length 13.7 mm, head length/SVL ratio 0.27; snout length 6.1 mm; head width 8.3 mm; longest toe of adpressed hind limb reaching to anterior margin of eye; shank length 13.0 mm, shank length/head length ratio 0.95; longest finger of extended forelimb reaching to tip of snout; longest finger of adpressed forelimb reaching a point 2.0 mm in front of anterior insertion of hind limbs. Dorsal head scales in snout region mostly keeled, other dorsal head scales smooth, keeled or rugose; 5 postrostrals; 6 scales between nasals; 2 prenasal scales on each side, the lower one in contact with both rostral and first supralabial; circumnasal separated from first supralabial by one scale; scales in distinct prefrontal depression mostly keeled; supraorbital semicircles well developed, narrowly in contact; supraorbital disc composed of an oval patch of 3 greatly enlarged scales; circumorbital row incomplete, therefore, on of the enlarged supraorbital scales broadly in contact with supraorbital semicircles; 2 elongated, strongly overlapping superciliaries, anterior one larger than posterior one, followed posteriorly by 3 to 5 keeled squarish scales of moderate size; about 4 rows of small keeled scales extending between enlarged supraorbitals and superciliaries; parietal depression shallow; interparietal scale well developed, 2.3 × 1.0 mm (length × width), surrounded by scales of moderate to large size; 2 scales present between interparietal and supraorbital semicircles; canthal ridge distinct, composed of 3 large and 3 small anterior canthal scales; 6 scales present between second canthals; 8 scales present between posterior canthals; 22 (right) – 21 (left) mostly keeled loreal scales in a maximum of 5 (right) – 4 (left) horizontal rows; 5 keeled subocular scales arranged in a

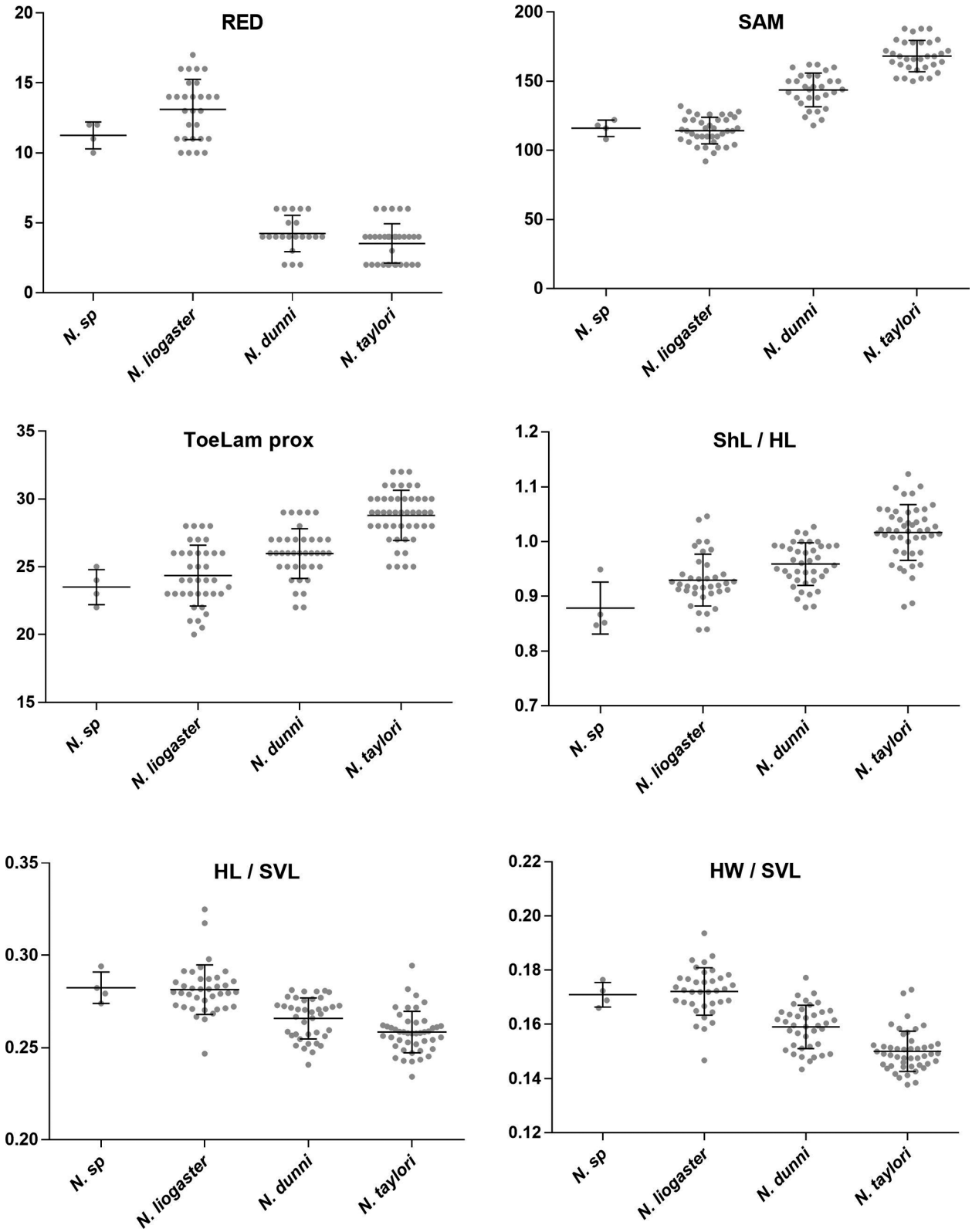

Fig. 4. Scatter plots illustrating morphological variation in the species related to *Norops liogaster*. *N.* sp. = the Espino Blanco specimens. For abbreviations see text.

single row; 6 supralabials to level below center of eye; 2 suboculars broadly in contact with 3 supralabials; ear opening 1.1 × 1.9 mm (length × height); mental distinctly wider than long, completely divided medially, bordered posteriorly by 3 postmentals, outer ones much larger than median one; 6 (right) – 7 (left) infralabials to level below center of eye; 2 (right) – 1 (left) greatly enlarged sublabials in contact with infralabials; keeled granular scales present on chin and throat; dewlap very large (187 mm^2), extending from level below anterior margin of eye to

Fig. 5. *Norops brianjuliani* (male holotype, SMF 96360) in life. Photograph by Raúl Gómez Trejo Pérez.

midbody; extended dewlap with 8–9 horizontal gorgetal-sternal rows containing 13–17 scales per row; dorsum of body with keeled, slightly mucronate, subimbricate scales; about 11 medial rows of greatly enlarged dorsal scales, transition between these middorsal and much smaller flank scales more or less abrupt; largest dorsal scales about 0.70 × 0.60 mm (length × width); about 24 medial dorsal scales in one head length; about 43 medial dorsal scales between levels of axilla and groin; lateral scales pointed granulars, juxtaposed to subimbricate and slightly heterogeneous in size, average size 0.20 mm in diameter; ventrals at midbody smooth, flat, imbricate with rounded posterior margins, slightly heterogeneous in size, about 0.60 × 0.65 mm (length × width); about 26 medial ventral scales in one head length; about 41 medial ventral scales between levels of axilla and groin; 122 scales around midbody; caudal scales keeled; middorsal caudal scales not enlarged, not forming a crest; lateral caudal scales without whorls of enlarged scales, although an indistinct division in segments is discernible; a pair of greatly enlarged postcloacal scales present, about 1.2 mm wide; no tube-like axillary pocket present; scales on dorsal surface of forelimb keeled, imbricate; digital pads dilated, dilated pad about 3 times width of non-dilated distal phalanx; distal phalanx narrower than and raised from dilated pad; 23 lamellae under phalanges II–IV of Toe IV of hind limbs; 7 scales under distal phalanx of Toe IV of hind limbs.

The almost completely everted hemipenis is a small unilobate organ; sulcus spermaticus bordered by poorly developed sulcal lips; no surface ornamentation discernable.

Coloration in life was recorded as follows: Dorsal ground color Cinnamon-Rufous (31) with a suffusion of Brussels Brown (33) medially and with a Robin Rufous (2) occipital marking; flanks with a Drab-Gray (256) longitudinal lateral stripe; dorsal surface of forelimbs Brick Red (36); ventral surfaces of head, body, limbs, and tail Light Buff (2) with suffusions of Beige (254); dewlap Magenta (236) with Pale Rose (76) suffusions around white gorgetals; iris Kingfisher Rufous (28).

Coloration after almost six years preservation in 70% ethanol was recorded as follows: Dorsal surfaces of head, body, and tail Drab (19) with a suffusion of Vandyke Brown (281) in vertebral region and base of tail; dorsal surfaces of limbs Tawny Olive (17); chin Beige (254); ventral surface of body Light Buff (2) with a suffusion of Drab (19); ventral surfaces of limbs and tail Light Buff (2); dewlap Fawn Color (258) with white gorgetals.

Variation. The paratypes agree well with the holotype in general appearance, morphometrics and scalation (see Table 1). Variation was evident in some scalation characters as follows: The number of greatly enlarged dorsal scale rows varies from 10 to 12. The number of scale rows separating the supraorbital semicircles from each other varies from 0 to 1. There is variation in the shape of the prenasal scales. In two of the paratypes (SMF 96361–62) the lower prenasal scale reaches to upper level of nostril on the right side, but only to center of

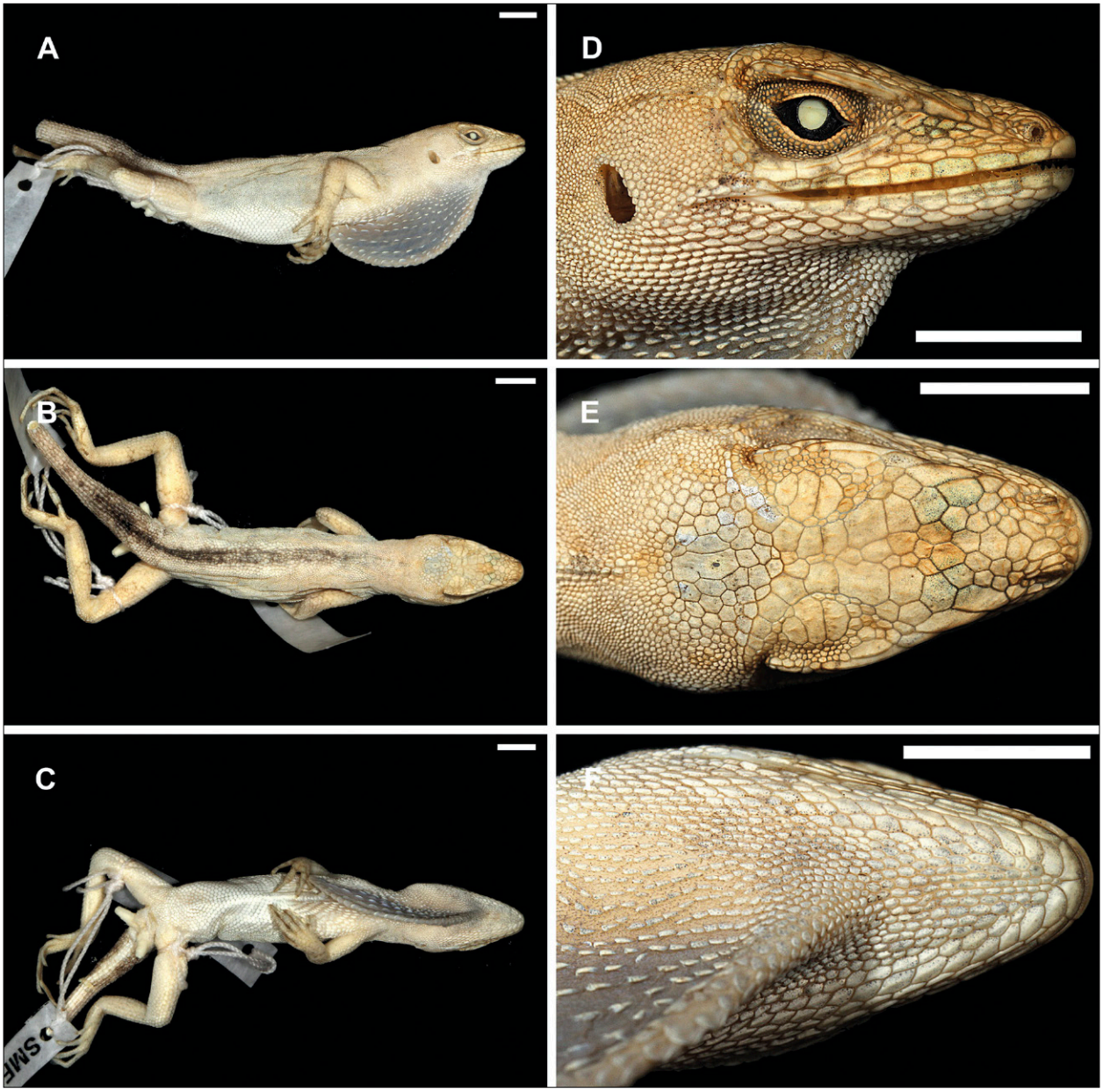

Fig. 6. Holotype of *Norops brianjuliani* (SMF 96360). Scale bars equal 10 mm in A–C and 5 mm in D–F. Photos by G.K.

nostril on the left side, whereas in SMF 96363 the prenasal reaches to upper level of nostril on both sides.

Etymology. In recognition of his contributions to the research and conservation of biodiversity, which includes his volunteer work, education of our youth, and efforts through the nonprofit BIOPAT initiative, we dedicate this newly discovered species of lizard to Brian Jeffrey Julian. Therefore, this anole is scientifically named *Norops brianjuliani* and may commonly be known as Brian's Anole.

Natural history notes. All type specimens were collected at night while the lizards were sleeping on low vegetation along the road, 0.5–1.5 m above the ground. The habitat in the vicinity of the type locality is montane pine-oak forest.

Geographic Distribution and Conservation. As currently known, *Norops brianjuliani* is restricted to the southern Sierra Madre del Sur in southern Guerrero (Fig. 8). Given the little we know about this species, we classify *N. brianjuliani* as Data Deficient based on the IUCN Red List Categories and Criteria (IUCN 2001).

Discussion

Norops brianjuliani is only known from a single locality in the Sierra Madre del Sur of southern Mexico. More field work is needed to evaluate the actual geographic distribution of this species. Although doubtless more widespread than currently known, this species is certainly a micro-endemic from the Pacific versant of this mountain

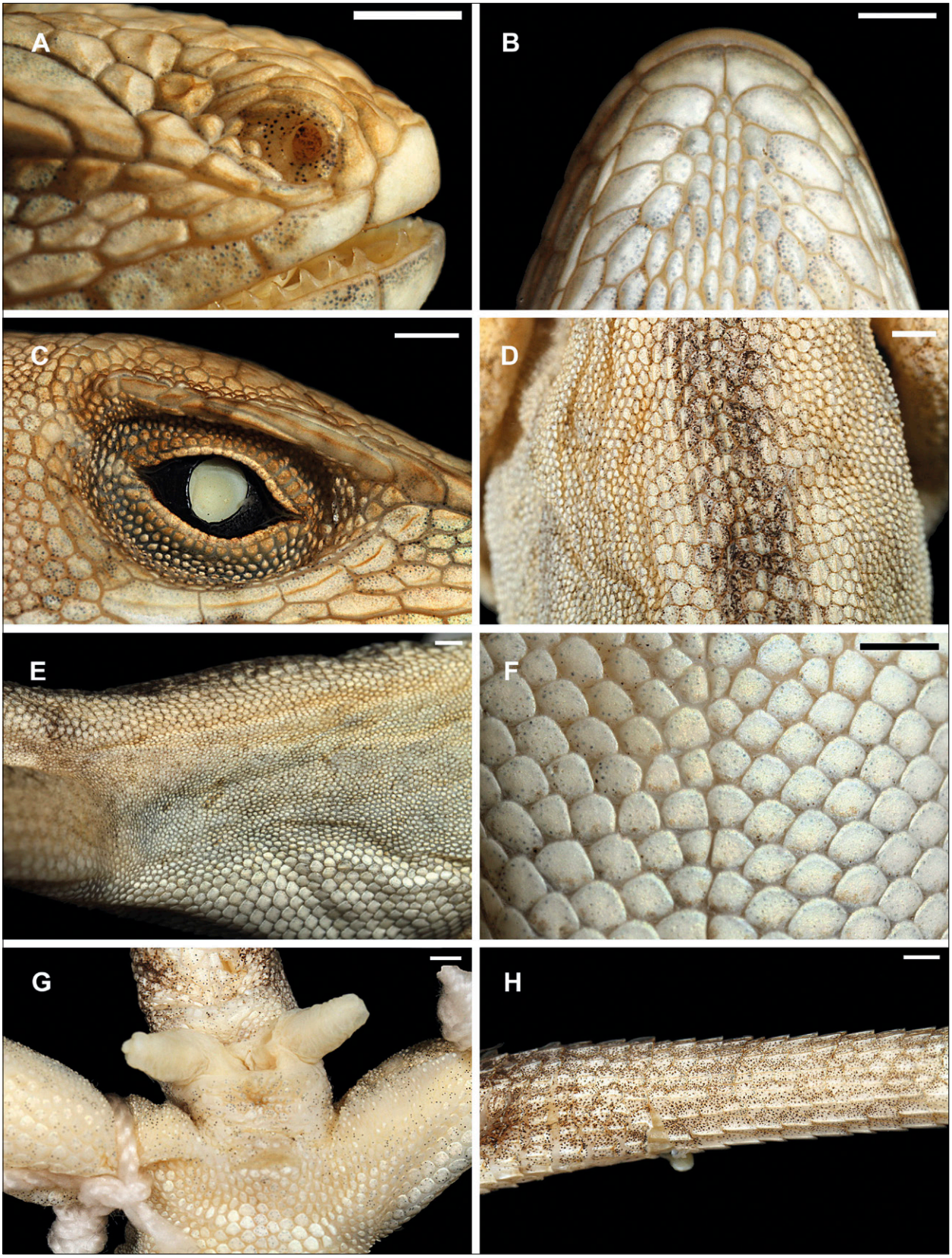

Fig. 7. Holotype of *Norops brianjuliani* (SMF 96360). (A) nasal region; (B) chin region; (C) superciliary region; (D) dorsal region; (E) flank region; (F) midventer; (G) cloacal region; (H) lateral view of tail. Scale bars equal 1.0 mm. Photos by G.K.

range. Also, it is likely that continued fieldwork will produce additional undescribed species from the pine-oak and cloud forests of this mega-diverse region.

Our results from the ABGD analysis support the species delimitation for most of the included taxa as proposed by Köhler *et al*. (2014a), except for the spe-

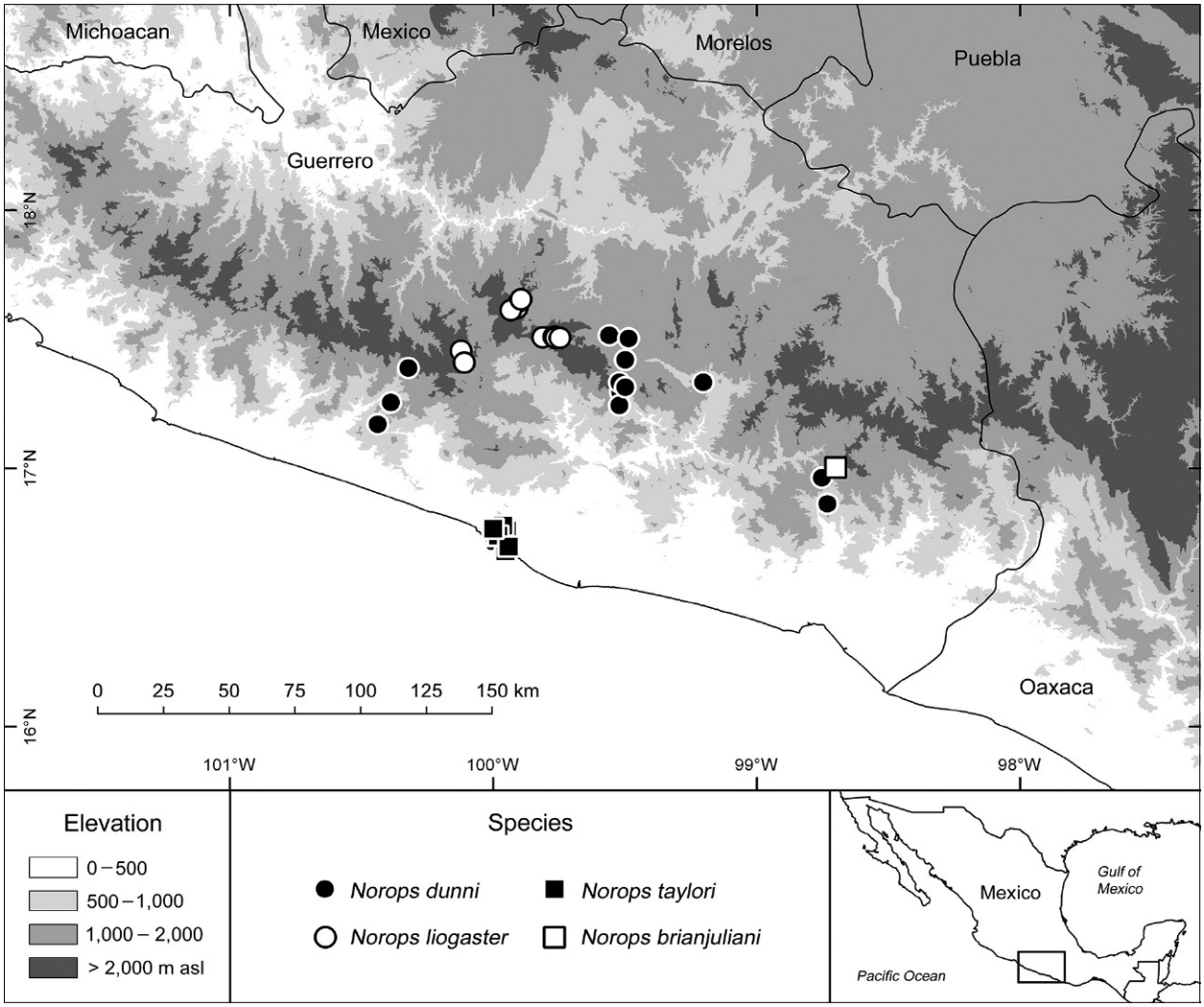

Fig. 8. Map indicating collecting localities of the species related to *Norops liogaster*. Each symbol can represent one or more adjacent localities.

cies pairs *N. boulengerianus* / *N. immaculogularis* and *N. dunni* / *N. taylori*, which this analysis suggests to be recognized as a single species, respectively. However, in all our trees, these taxa form monophyletic groups separated by modest genetic distances (16S / COI: *N. boulengerianus* / *N. immaculogularis*: 1.9% / 7.1%; *N. dunni* / *N. taylori*: 2.2% / 6.0%). Furthermore, differences in external morphology (i.e., male dewlap coloration, body size) between the nominal species of these pairs have been documented (KÖHLER *et al*., 2014a). Therefore, we tentatively continue to recognize these nominal taxa as distinct species.

Acknowledgments

Collecting and exportation permits were issued by Martin Vargas Prieto, Secretaria del Medio Ambiente y Recursos Naturales, México D.F., Mexico. For the loan of and/or access to specimens, we thank Alan Resetar, Field Museum of Natural History (FMNH), Chicago; Victor Hugo Reynoso, Instituto de Biología (IBH), Universidad Nacional Autónoma de México, México D.F.; William E. Duellman and John E. Simmons, University of Kansas, Natural History Museum (KU), Lawrence; James Hanken, Jonathan Losos, and José P. Rosado, Museum of Comparative Zoology, Harvard University (MCZ), Cambridge; Christopher N. Phillips and Daniel B. Wylie, Illinois Natural History Survey, University of Illinois (UIMNH), Champaign; Ronald N. Nussbaum and Greg Schneider, University of Michigan Museum of Zoology (UMMZ), Ann Arbor; Ron W. McDiarmid and W. Ronald Heyer, National Museum of Natural History (USNM), Washington, D.C.; and J. Campbell and C. Franklin, The University of Texas at Arlington (UTA), Arlington. We thank Linda Mogk, Senckenberg Research Institute, Frankfurt, for doing the molecular lab work that resulted in the new DNA sequences included in this contribution. For field assistance, we thank Raúl Gómez Trejo Pérez. In 2012, GK received an Ernst Mayr Travel Grant in Animal Systematics from the MCZ and a Visiting Scholarship Award from the FMNH, which enabled him to examine relevant Mexican anoles in the collections of these institutions.

References

Bouckaert, R. R. & Heled, J. (2014). densitree 2, Seeing trees through the forest. *BioRxiv*, doi.org/10.1101/012401

Burnham, K. P. & Anderson, D. R. (2002). *Model Selection and Multimodel Inference, A Practical Information-Theoretic Approach*, 2nd edition. New York, Springer.

Castañeda, M. D. R. & de Queiroz, K. (2013). Phylogeny of the *Dactyloa* clade of *Anolis* lizards: new insights from combining morphological and molecular data. *Bulletin of the Museum of Comparative Zoology*, **160**, 345–398.

de Queiroz, K. (2007). Species concepts and species delimitation. *Systematic Biology,* **56**, 879–886.

Drummond, A. J., Ashton, B., Cheung, M., Heled, J., Kearse, M., Moir R. *et al*. (2010) geneious v.4.8.5. (www.geneious.com; accessed 10 November 2011).

Drummond, A. J., Suchard, M. A., Xie, D. & Rambaut, A. (2012). Bayesian phylogenetics with beauti and the beast 1. 7. *Molecular Biology and Evolution*, **29**, 1969–1973.

Edgar, R. C. (2004). muscle: a multiple sequence alignment method with reduced time and space complexity. *BMC Bioinformatics*, **5**, 1–19.

Etheridge, R. (1959). *The Relationships of the Anoles* (*Reptilia, Sauria, Iguanidae*). *An Interpretation Based on Skeletal Morphology*. PhD. Dissertation, University of Michigan, Ann Arbor.

Gelman, A. G. & Rubin, D. B. 1992. Inference from iterative simulation using multiple sequences. *Statistical Science*, **7**, 457–472.

Glez-Peña, D., Gómez-Blanco, D., Reboiro-Jato, M., Fdez-Riverola, F. & Posada, D. (2010). ALTER, program-oriented format conversion of DNA and protein alignments. *Nucleic Acids Research*, **38**, 14–18.

Guindon, S., Dufayard, J., Lefort, V., Anisimova, M., Hordijk, W. & Gascuel, O. (2010). New algorithms and methods to estimate maximum-likelihood phylogenies, assessing the performance of PhyML 3. 0. *Systematic Biology*, **59**, 307–321.

Huelsenbeck, J. P. & Ronquist, F. (2001). mrbayes, Bayesian inference of phylogenetic trees. *Bioinformatics*, **17**, 754–755.

Ivanova, N. V.; De Waard, J.; Hebert, P. D. N. (2006). An inexpensive, automation-friendly protocol for recovering high-quality DNA. *Molecular Ecology Notes*, **6**, 998–1002.

IUCN (2001). IUCN Red List Categories and Criteria, Version 3. 1. IUCN Species Survival Commission, Gland, Switzerland and Cambridge, UK. Available from, http//www.iucnredlist.org/documents/redlist_cats_crit_en.pdf (accessed 17 April 2013).

Kekkonen, M., Mutanen, M., Kaila, L., Nieminen, M. & Hebert, P. D. N. (2015). Delineating species with DNA barcodes, a case of taxon dependent method performance in moths. *PLoS ONE*, **10**, e0122481.

Köhler, G. (2012). *Color Catalogue for Field Biologists*. Offenbach, Herpeton.

Köhler, G. (2014). Characters of external morphology used in *Norops* taxonomy– –Definition of terms, advice on usage, and illustrated examples. *Zootaxa*, **3774**, 201–257.

Köhler, G., Batista, A., Vesely, M., Ponce, M., Carrizo, A. & Lotzkat, S. (2012). Evidence for the recognition of two species of *Norops* formerly referred to as *A. tropidogaster* (Squamata, Dactyloidae). *Zootaxa,* **3348**, 1–23.

Köhler, G., Gómez Trejo Pérez, R., Petersen, C. B. P. & Méndez de la Cruz, F. R. (2014a). A revision of the Mexican *Norops* (Reptilia, Squamata, Dactyloidae) from the Pacific versant west of the Isthmus de Tehuantepec in the states of Oaxaca, Guerrero, and Puebla, with the description of six new species. *Zootaxa*, **3862**, 1–210.

Köhler, G., Townsend, J. H. & Petersen, C. B. P. (2016). A taxonomic revision of the *Norops tropidonotus* complex (Squamata, Dactyloidae), with the resurrection of *N. spilorhipis* (Álvarez del Toro and Smith, 1956) and the description of two new species. *Mesoamerican Herpetology*, **3**, 8–41.

Köhler, G., Vargas, J. & Lotzkat, S. (2014b). Two new species of the *Norops pachypus* complex (Squamata, Dactyloidae) from Costa Rica. *Mesoamerican Herpetology*, **1**, 254–280.

Kumar, S., Stecher, G. & Tamura, K. (2016). mega7, Molecular Evolutionary Genetics Analysis version 7. 0 for bigger datasets. *Molecular Biology and Evolution*, **33**, 1870–1874.

Lanfear, R., Frandsen, P. B., Wright, A. M., Senfeld, T. & Calcott, B. (2016). PartitionFinder 2, new methods for selecting partitioned models of evolution for molecular and morphological phylogenetic analyses. *Molecular Biology and Evolution*, **34**, 772–773.

Lotzkat, S., Bienentreu, J. -F., Hertz, A. & Köhler, G. (2011). A new species of *Norops* (Squamata, Iguania, Dactyloidae) formerly referred to as *A. pachypus* from the Cordillera de Talamanca of western Panama and adjacent Costa Rica. *Zootaxa,* **3125**, 1–21.

Mayrose, I., Friedman, N. & Pupko, T. (2005). A gamma mixture model better accounts for among site rate heterogeneity. *Bioinformatics*, **21**, ii151–ii158.

Minh, B. Q., Nguyen, M. A. T. & von Haeseler, A. (2013). Ultrafast approximation for phylogenetic bootstrap. *Molecular Biology and Evolution*, **30**, 1188–1195.

Nicholson, K. E., Crother, B. I., Guyer, C. & Savage, J. M. (2012). It is time for a new classification of anoles (Squamata, Dactyloidae). *Zootaxa*, **3477**, 1–108.

Nicholson, K. E., Crother, B. I., Guyer, C. & Savage, J. M. (2014). Anole classification: a response to Poe. *Zootaxa*, **3814**, 109–120.

Nicholson, K. E., Crother, B. I., Guyer, C. & Savage, J. M. (2018). Translating a clade based classification into one that is valid under the international code of zoological nomenclature, the case of the lizards of the family Dactyloidae (order Squamata). *Zootaxa*, **4461**, 573–586.

Ogilvie, H. A., Bouckaert, R. R. & Drummond, A. J. (2017). starbeast2 brings faster species tree inference and accurate estimates of substitution rates. *Molecular Biology and Evolution*, **34**, 2101–2114.

Poe, S. (2004). Phylogeny of anoles. *Herpetological Monographs*, **18**, 37–89.

Poe, S. (2013). 1986 Redux, New genera of anoles (Squamata, Dactyloidae) are unwarranted. *Zootaxa*, **3626**, 295–299.

Poe, S., Nieto-Montes de Oca, A., Torres-Carvajal, O., de Queiroz, K., Velasco, J. A., Truett, B., Gray, L. N., Ryan, M. J., Köhler, G., Ayala-Varela, F. & Latella, I. (2017). A phylogenetic, biogeographic, and taxonomic study of all extant species of *Anolis* (Squamata; Iguanidae). *Systematic Biology*, **66**, 663–697.

Puillandre, N., Lambert, A., Brouillet, S. & Achaz, G. (2012). ABGD, Automatic Barcode Gap Discovery for primary species delimitation. *Molecular Ecology*, **21**, 1864–1877.

Ronquist F. & Huelsenbeck, J. P. (2003). mrbayes 3, bayesian phylogenetic inference under mixed models. *Bioinformatics*, **19**, 1572–1574.

Sabaj Pérez, M. H. (2016). Standard symbolic codes for institutional resource collections in herpetology and ichthyology. An online reference. Version 6.5 (16 August 2016). Available from http://www.asih.org (accessed 19 October 2018).

Sullivan, J., Swofford, D. L. & Naylor, G. J. P. (1999). The effect of taxon sampling on estimating rate heterogeneity parameters of maximum-likelihood models. *Molecular Biology and Evolution*, **16**, 1347–1356.

Tamura, K., Stecher, G., Peterson, D., Filipski, A, & Kumar, S. (2013). mega6: Molecular Evolutionary Genetics Analysis version 6.0. *Molecular Biology and Evolution,* **30**, 2725–2729.

Trifinopoulos, J., Nguyen, L.-T., von Haeseler, A. & Minh, B. Q. (2016). w-iq-tree, a fast online phylogenetic tool for maximum likelihood analysis. *Nucleic Acids Research*, **44**, W232–W235.

Yang, Z. (2006). *Computational Molecular Evolution*. *Oxford Series in Ecology and Evolution*. Oxford, Oxford University Press.

Yang, Z. Landry, J.-F. & Hebert, P. D. N. (2016). A DNA barcode library for North American Pyraustinae (Lepidoptera: Pyraloidea: Crambidae). *PLoS ONE*, **11**, e0161449.

ZooBank registration

This published work and the nomenclatural acts it contains have been registered in ZooBank, the online registration system for the International Commission on Zoological Nomenclature (ICZN). The ZooBank LSIDs (Life Science Identifiers) can be resolved and the associated information can be viewed through any standard web browser by appending the LSID to the prefix http://zoobank.org. The LSID for this publication is as follows: urn:lsid:zoobank.org:pub:F79A90CE-EBBB-427D-9174-947244D11365.

Appendix 1

Comparative Specimens Examined

Anolis dunni — **Mexico:** Guerrero: Acahuizotla: KU 87309, MCZ R-78696–98, USNM 47753; Agua de Obispo: FMNH 116751, IBH 26591–92, KU 87306–08, MCZ R-78722–23, SMF 96194, 96371–72, 96379–81; near Agua de Obispo, Km 350–351: UIMNH 20125; Chilpancingo: SMF 96238–39; Malpais, S of Chilpancingo: UIMNH 20126; Petaquillas near Chilpancingo: IBH 26589–90, SMF 96252–54; 1 mi SW Colotlipa: MCZ R-78719–21; Presa El Molino near Tixtla: IBH 26611, 26594, SMF 96255–56; 7.1 mi S Puerto Gallo: UMMZ 130983; 19.2 mi S Puerto Gallo: UMMZ 130984; 8.6 mi (by road) N from San Vicente: UTA R-4178.

Anolis liogaster — **Mexico:** Guerrero: 17.2 mi W Asoleadero: UMMZ 130982; Pueblo los Morros, 62.8 km from Zumpango del Rio via Casa Verde: UMMZ 229862, 229867; W of Chilpanzingo, between the villages Filo de Caballo y Carrizal: UMMZ 229869; 37.7 km SW Filo de Caballo: KU 182540–42; Omiltemi: FMNH 108508, 125620–21, 125624, IBH 26599–601, 26605–06, MCZ R-85021–22, SMF 96199–206, USNM 47748–51, 148865; 1.4 mi W Patio de Aviacion: UMMZ 130981.

Anolis omiltemanus — **Mexico:** Guerrero: 15 mi W Asoleadero: UMMZ 130985; La Laguna near Omiltemi: IBH 26554–57, 26559; SMF 96226–30; 0.5–1.0 m S Omiltemi: UTA R-4408; 1.0 mi E Omiltemi: UTA R-4409.

Anolis peucephilus — **Mexico:** Oaxaca: ca. 27 km on road N San Gabriel Mixtepec, 1325 m: SMF 96368–69; ca. 28 km on road N San Gabriel Mixtepec, 1400 m: GK-4138 (IBH), 4467 (IBH), SMF 96241; ca. 27.5 km on road N San Gabriel Mixtepec, 1380 m: SMF 96370; on road from San Gabriel Mixtepec to El Vidrio, 1924 m: SMF 96725.

Anolis taylori — **Mexico:** Guerrero: Acapulco: USNM 132358–61; Acapulco, Jardin Botanico: IBH 26597, 26602–03, SMF 96268–74; Acapulco, zona arqueologica Palma Sola: IBH 26595–98, 26604; mountains near Acapulco: FMNH 116741–43, 116746–48, 116750, 116752, 116754–56, 116759, 116762–65, 116767, MCZ R-58225–26, UIMNH 20099, 200101–02, 200104, 200106; 0.5 mi S Las Cruces: KU 320889–93; 1 mi W Puerto Marqués: KU 320902–08.

Appendix 2

GenBank accession numbers of specimens included in molecular analyses

Voucher #	species	16S	COI
IBH 26990	*Norops boulengerianus*	KP178221	KP231855
SMF 96197	*Norops boulengerianus*	KP178219	KP231800
SMF 96386	*Norops boulengerianus*	KP178222	KP231856
SMF 96360	*Norops brianjuliani*	MK621405	MK629716
SMF 96361	*Norops brianjuliani*	MK621406	MK629717
SMF 96362	*Norops brianjuliani*	MK621407	MK629718
SMF 96363	*Norops brianjuliani*	MK621408	MK629719
IBH 26588	*Norops dunni*	KP178225	KP231781
IBH 26591	*Norops dunni*	KP178235	KP231828
IBH 26592	*Norops dunni*	KP178234	KP231827
IBH 26593	*Norops dunni*	KP178226	KP231795
SMF 96191	*Norops dunni*	KP178228	KP231797
IBH 26563	*Norops immaculogularis*	KP178252	KP231801
SMF 96265	*Norops immaculogularis*	KP178254	KP231802
IBH 26599	*Norops liogaster*	KP178259	KP231787
IBH 26601	*Norops liogaster*	KP178261	KP231790
IBH 26605	*Norops liogaster*	KP178260	KP231788
IBH 26607	*Norops liogaster*	KP178258	KP231786
IBH 26503	*Norops megapholidotus*	KP178267	KP231785
IBH 26504	*Norops megapholidotus*	KP178268	KP231791
SMF 96211	*Norops megapholidotus*	KP178266	KP231780
SMF 96212	*Norops megapholidotus*	KP178269	KP231829
IBH 26573	*Norops microlepidotus*	KP178272	KP231826
SMF 96213	*Norops microlepidotus*	KP178270	KP231821
SMF 96382	*Norops microlepidotus*	KP178242	KP231846
SMF 96384	*Norops microlepidotus*	KP178244	KP231847
IBH 26508	*Norops nebuloides*	KP178284	KP231814
IBH 26515	*Norops nebuloides*	KP178287	KP231816
IBH 26516	*Norops nebuloides*	KP178288	KP231817
IBH 26519	*Norops nebuloides*	KP178289	KP231818
SMF 96218	*Norops nebuloides*	KP178285	KP231815
IBH 26551	*Norops nebulosus*	MK621402	—
SMF 96221	*Norops nebulosus*	MK621403	—
SMF 96224	*Norops nebulosus*	MK621404	—
SMF 96393	*Norops nietoi*	KP178297	KP231833
SMF 96394	*Norops nietoi*	KP178298	KP231834
SMF 96406	*Norops nietoi*	KP178305	KP231839
IBH 26554	*Norops omiltemanus*	KP178346	KF990246
IBH 26555	*Norops omiltemanus*	KP178345	KF990247
IBH 26556	*Norops omiltemanus*	KP178344	KF990248
IBH 26557	*Norops omiltemanus*	KP178347	KF990245
IBH 26559	*Norops omiltemanus*	KP178349	KF990243
SMF 96230	*Norops omiltemanus*	KP178348	KF990244
GK-4138	*Norops peucephilus*	KP178351	—
SMF 96241	*Norops peucephilus*	KP178350	—
SMF 96369	*Norops peucephilus*	KP178352	—
SMF 96440	*Norops quercorum*	KP178315	KP231848
SMF 96443	*Norops quercorum*	KP178316	KP231849
SMF 96445	*Norops quercorum*	KP178317	KP231850
SMF 96449	*Norops quercorum*	KP178318	KP231851
SMF 96450	*Norops quercorum*	KP178319	KP231852

Appendix 2 continued.

IBH 26517	*Norops stevepoei*	KP178277	KP231808
SMF 96245	*Norops stevepoei*	KP178280	KP231810
IBH 26566	*Norops subocularis*	KP178330	KP231778
SMF 96258	*Norops subocularis*	KP178331	KP231779
SMF 96262	*Norops subocularis*	KP178334	KP231794
IBH 26568	*Norops subocularis*	MK621409	KP231782
IBH 26595	*Norops taylori*	KP178343	KP231777
IBH 26597	*Norops taylori*	KP231775	KP231775
IBH 26598	*Norops taylori*	KP178342	KP231776
IBH 26603	*Norops taylori*	KP178340	KP231773
SMF 96273	*Norops taylori*	KP178341	KP231774
IBH 26513	*Norops zapotecorum*	KP178290	KP231819
IBH 26582	*Norops zapotecorum*	KP178291	KP231820
SMF 96247	*Norops zapotecorum*	KP178282	KP231811
SMF 96248	*Norops zapotecorum*	MK621410	KP231812
n.a.	*Basiliscus vittatus*	AB218883	AB218883